Rakenteiden Mekaniikka (Journal of Structural Mechanics)
Vol. 56, No. 1, 2023, pp. 51–61
http://rakenteidenmekaniikka.journal.fi
https://doi.org/10.23998/rm.124815


VERTAISARVIOITU
KOLLEGIALT GRANSKAD
PEER-REVIEWED
www.tsv.fi/tunnus

# Characterising the notch root radii and analyses of stress concentration factors near the dominant valleys of rough surface profiles

Silas Z. Gebrehiwot, Heikki Remes, Leonardo Espinosa-Leal and Marinus Vermunt

**Summary** Surface roughness is one of the key surface integrity factors affecting the strength and fatigue life of components. Stress concentrations occur due to the randomness of the surface profiles. The presence of a dominant valley, a complex geometry and interacting effects exasperate the severity of the stress concentrations. To estimate the theoretical stress concentration factor (SCF) at the valley, the notch root radius should be estimated carefully. We propose an effective method for estimating the root radius of the deepest valley using numerical derivative techniques. The surface roughness of a carefully sanded Alumec 89 block was measured using SJ-400 tester. The 1-D roughness data was used first to evaluate the root radius of the deepest valleys and then, estimate the SCF using analytical and computational methods. We used 2-D finite element (FE) models under uniaxial tension for the computational analyses. The validity of our method is based on determining the SCF using different theoretical methods and comparing the results to the FE calculations. The theoeritical estimations are made using the Neuber, Inglis and Arola-Ramulu approaches, whereas COMSOL Multiphysics is used for the FE analyses. Comparing the theoeritical methods with the FE calculations, the Arola-Ramulu approach was better, with a maximum of 16.3 % error. The minimum deviations can be explained by the model containing parameters such as $R_y$, $R_z$ and $R_a$ which are inherent to the roughness profile of the material.

*Keywords:* root radius, stress concentration factor, surface roughness, fatigue notch factor

*Received: 24 November 2022. Accepted: 3 May 2023. Published online: 12 June 2023.*

## Introduction

The surface integrity of materials is affected by microstructural defects, residual stress and surface roughness that stem from the manufacturing processes. The study of surface integrity influence on fatigue life of a material is a complex phenomenon due to the coexistence of different surface integrity factors [1]. The coexistence affects the fatigue property of materials due to the detrimental effect caused to the surface layers. Few studies on machined components suggest that the fatigue properties are influenced by the existence of surface roughness and microstructural inclusions. For instance, a study by Gao and Li on unpolished 40CrNi2Si2MoVA steel indicated a 10% decrease of fatigue limit due to surface roughness [2].

[1]Corresponding author: silas.gebrehiwot@arcada.fi

Similarly, intense thermal and rapid machining operations introduce microstructural alterations that affect the mechanical, metallurgical and chemical properties [3]. Recent studies show that the ISO standard for correlations between surface roughness and fatigue limit does not hold for fatigue test results, see e.g., [4], [5]. Based on these studies, the fatigue limit of a rough surface has increased beyond the estimations set by the ISO standard of correlations for acceptable limits of surface roughness.

Accurate characterisation of surface roughness contributes to a better understanding of the underlying relationship between surface roughness and stress concentration. The randomness of the roughness profile results in a complex state of surface stresses which arise from the interaction effect [6–8]. Based on the geometries and orientation of the roughness, the stress concentration interactions could be detrimental or mitigating. Murakami [8] showed that a rough surface generally has higher stress concentrations. However, the extent of influence may depend on the depth and width of a pitch between consecutive roughness profiles. Compacted pitches usually develop an interacting effect that mitigates stress concentration, whereas wider pitches give rise to relatively higher stress concentration [8]. Theoretically, SCF is usually evaluated as the stress ratio between the local and nominal ones [9]. The formulation is based on the classical linear elasticity theory at macro-scale, hence size-independent. To the contrary, the measurement and characterisation of surface roughness is usually at micrometre-scale. Therefore, the severity of stress concentration will become additionally size-dependent, see the work by Khakalo and J. Niiranen [10] on the gradient-elastic stress analysis of an infinite plate. The relationship between fatigue strength and surface roughness has been studied by a number of researchers. Majority of the analyses have been conducted using experimental methods. There are only few analytical methods on characterizing the stress concentrations of a roughness surface. A semi-empirical formulation proposed by Neuber as well as a material dependent formulation by Arola and Ramulu are widely used in SCF estimations [11].

The influence of surface roughness on the fatigue of 7010 aluminium alloy is studied in [12]. The severity of surface roughness on creating localized stress concentrations and the contributions to crack propagation are studied by modelling filtered 1D roughness profile on FE. However, the machined surface profile is shallow, and the filtering process reduces the stochasticity that could misrepresent the surface details. Arola D. [13] studied the influences of net-shape machining on the surface texture of Fiber Reinforced plastic (FRP). The surface textures are further related to the material's flexural strength via theoeritical SCF calculations. Surface topology is characterised by a profile moment that is modelled using superimposed micro-cosine shaped functions [14]. The second profile moment is used to estimate the SCF analytically and, validated using FE model. Similarly, analytical approach is proposed to estimate SCF for a slightly rough surface modelled using superposition of numerous cosine function via Fourier series [15]. However, the series of cosine functions again could misrepresent the inherent randomness of the real surface profiles.

Many scholars focus on characterising surface roughness of materials in relation to SCF estimations [11–16]. However, most of the works do not consider the local stochasticity of the roughness as well as the severity stress concentrations near of dominant valley regions that lead to fatigue related failures. Therefore, our objective is to evaluate the notch radius of the deepest valleys measured using SJ-400 profilometer. And for the purpose, the surface roughness of the high strength aluminium alloy, Alumec 89, is measured at different locations according to ISO 4287 standard. Based on the calculated notch radii, the SCFs are evaluated theoretically using the Neuber, Arola-Ramulu and Inglis approaches. The theoretical findings are compared with the results of the FE analyses.

## Theories of surface roughness and stress concentrations

### *Surface roughness*

Surface roughness consists of irregularities that remain on the surface after a material passes through certain manufacturing processes [17]. The irregularities affect the performances of components in mechanical applications. These irregularities are characterised by peaks and valleys of the surface profile. The localized peaks are termed as asperities [18]. The manufacturing and machining processes generate surface roughness due to the forming or other subtractive operations. The surface roughness scale has a wide range of dimensions from steps of 20 mm in traverse to size of interatomic distances of tenths of a micron [17]. The surface profiles that are in the scale of microroughness can be random, or repetitive with variety of localized peaks and troughs [19]. The irregularities of surface roughness result in complex geometry of surface topology that requires detailed assessment to describe the textures and thus, their influence on stress concentrations.

The Surface roughness of materials is characterized by a variety of amplitude and spacing parameters [20]. Some of the amplitude parameters include arithmetic mean, $R_a$, maximum height of the profile, $R_y$, maximum profile depth, $R_v$ and so forth [21]. Measured from the mean line, the arithmetic mean height parameter is

$$R_a = \frac{1}{L}\int_0^L |z| dx. \tag{1}$$

In Eq. (1), $z$ is the height of the profile, whereas $L$ is the length of the roughness profile evaluated. On the other hand, the maximum height of the profile is

$$R_y = R_v + R_p. \tag{2}$$

In Eq. (2), the $R_p$ is the peak height of the roughness whereas, $R_v$ is the maximum valley measured from the mean line. The ten-point height is average value of the five highest peaks and five deepest valleys of the roughness profile. That is

$$R_z = \frac{1}{5}\left[\sum_{i=1}^{5}\left(R_{pi} + R_{vi}\right)\right]. \tag{3}$$

### *Stress concertation factors for rough surface profiles*

Machineries, vehicles, ships and airliners have numerous components which contain stress concentrations due to their geometrical nonuniformity. Stress concentration is defined as a localized phenomenon of higher stress near geometrical changes which are beyond the nominal stress value [9]. Geometrical discontinuities occur in many forms such as surface notches or subsurface defects, having a variety of geometric shapes. The discontinuities can reduce the fatigue life of materials. The general formula for the theoretical SCF, $K_t$, is presented as follows

$$K_t = \frac{\sigma_{max}}{\sigma_{nom}}. \tag{4}$$

In Eq. (4), $\sigma_{max}$ is the maximum stress at the geometrical change and, $\sigma_{nom}$ is the nominal stress at remote. The theoretical stress concentration in Eq. (4) does not consider geometrical entities of the discontinuities. However, the stress distribution around surface notches depends

on the radius of curvature which is a geometrical entity. Using elliptical coordinates and complex variables analyses, Inglis proposed SCF for an elliptical notch geometry [22]. With a major radius, $a$, minor radius, $b$, and notch root radius, $\rho$, Inglis suggested that

$$k_t = 1 + 2\frac{a}{b} = 1 + 2\sqrt{\frac{a}{\rho}}. \tag{5}$$

Eq. (5) is referred to as an equivalent ellipse method where the notches or grooves are approximated to an elliptical geometry. However, this method is applicable for shallow profiles that can be approximated to an elliptical geometry [16] and, used for isolated surface notch or subsurface geometries [9]. To the contrary, surface roughness is inherently random and continuous profile. The SCF analyses by Neuber and Arola-Ramulu consider some of the surface roughness parameters. The Neuber's approach is a semi-empirical model that involves the ten-point height parameter, $R_z$, and a notch root radius, $\rho$ [11]. The theoretical SCF suggested by Neuber is

$$k_t = 1 + n\sqrt{\lambda\frac{R_z}{\rho}}. \tag{6}$$

In Eq. (6), $n$ implies the loading mode and $\lambda$ is the ratio between the horizontal spacing and the asperities. The $n$ is valued 1 for shear and 2 for tension loadings. Alternative analytical approach is suggested by Arola-Ramulu [11,13] to estimate the SCF of a rough surface profile. The method incorporates the use of dominant profile valley and the average valley radius. Comparing to Neuber's, it has the arithmetic mean, $R_a$, and the maximum height profile parameter, $R_y$ additionally. The effective SCF by Arola-Ramulu is

$$\bar{k}_t = 1 + n\frac{R_a}{\bar{\rho}}\frac{R_y}{R_z}. \tag{7}$$

In Eq. (7) $n$ represents the mode of the loading, whereas, $\bar{\rho}$ is an effective profile valley radius and represents the average radius for dominant profile valleys [11].

## Methods

### *Modelling the root radius of the deepest valley profile*

The deep valley regions of the roughness can sometimes be the locations of higher stress concertation for in-plane loadings. The expressions given by Eqs. (5)–(7) can be used to estimate the SCF theoretically. Some of the terms in these equations can be directly obtained from surface roughness measurements except for the notch root radius. Therefore, we propose a numerical derivation method to evaluate the notch root radius of the deepest valley. The notch root radius $\rho$ is the inverse of the curvature $\varphi$ at dominant valley, and is given as

$$\rho = \frac{1}{\varphi} = \frac{1}{\frac{1}{L}\int_0^L \frac{\frac{d^2z}{dx^2}}{\left[1+\left(\frac{dz}{dx}\right)^2\right]^{3/2}}dx}. \tag{8}$$

To evaluate the notch root radius, we created 3 equidistant spacings to the left and right sides of the deepest valley. Therefore, we obtained a total of 7 z-coordinates between $z_{-3}$ and $z_{+3}$. Then, we evaluated the first and second order derivatives of $z$ using the central difference numerical derivative techniques. In the numerical differentiation, the Lagrange polynomial interpolation is used to perform a first order and second order derivatives of the data points given as $\left(x_{-j}, f\left(x_{-j}\right)\right)$, ... $\left(x_{-1}, f(x_{-1})\right), \left(x_0, f(x_0)\right)$ ... $\left(x_k, f(x_k)\right)$ [23]. Ignoring the truncation error, the first order numerical derivatives at $x_0$ is given as

$$f'(x_0) \approx \sum_{i=-j}^{k} f(x_i)\mathcal{L}'_{n,i}(x_0). \tag{9}$$

In Eq. (9), $\mathcal{L}'_{n,i}(x_0)$ is the derivative of the Lagrange polynomial at $x_0$. And $n$ represents the total points considered, $n = j + k + 1$. The derivative of the Lagrange polynomial at $x_0$ is

$$\mathcal{L}'_{n,i}(x_0) = \sum_{m \neq i} \frac{1}{x_i - x_m} \prod_{n \neq (i,m)} \frac{x_0 - x_n}{x_i - x_n}. \tag{10}$$

The second order numerical differentiation of the data points follows a similar process, with the approximate derivation at $x_0$ becoming

$$f''(x_0) \approx \sum_{i=-j}^{k} f(x_i)\mathcal{L}''_{n,i}(x_0). \tag{11}$$

In Eq. (11), the second order derivative of the Lagrange polynomial is

$$\mathcal{L}''_{n,i}(x_0) = \sum_{m \neq i} \frac{1}{x_i - x_m} \sum_{u \neq (i,m)} \frac{1}{x_i - x_u} \prod_{n \neq (i,m,u)} \frac{x_0 - x_n}{x_i - x_n}. \tag{12}$$

In the numerical derivatives, the $x_i$ are the $x$-coordinate data points that define the spacing between subsequent height profiles, which are given by $f(x_i)$, see the surface roughness of the first measurement in Fig. 1. We measured the surface roughness at three different locations and labelled them as measurement 1, measurement 2 and, measurement 3.

The root radius of the deepest valley in Fig. 1 is calculated by first taking equidistant horizontal spacings, $x_{i+1} - x_i = h_i$ and evaluating the first and second order numerical derivatives at $x_0 = 1.56$ mm for the case of measurement 1. The central derivatives are evaluated using Eqs. (9) and (11) and the root radius using Eq. (8). Our approach uses the geometrical correlation between curvature and radius to determine the values of the root radii for the deepest valleys. Fig. 2 shows the geometrical correlation and the local data points used for evaluations.

The root radii are evaluated by taking the height distributions within the limits of $x_{-3}$ and $x_{+3}$ horizontal spacings. The evaluations should provide reasonable value of a root radius that characterises the deepest valley section. Therefore, we made subsequent evaluations by altering the steps of increments on the horizontal spacings, $h_i$. The evaluated root radii for the different spacings are presented in Fig. 3.

Fig. 3 shows the relationship between the horizontal spacings and the calculated radii of the three measurements. For the horizontal spacings, $h_i < 0.1$ mm, the calculated radii are high and do not provide reasonable values within the limits of the standard roughness parameters measured. For example, the notch radius of the deepest valley at $h_i = 0.005$ mm is 111.09 μm for measurement 1. This notch radius is higher than the $R_t$, $R_a$ $R_v$ and $R_z$ values determined

for the measurement. Similar behaviours are observed for horizontal spacings, $h_i >$ 0.2 mm. For all the measurements, the minimum radii are found when the horizontal spacings are between 0.01mm and 0.02 mm. We used the minimum notch radii calculated in the SCF estimations. The SCFs are calculated using the analytical methods proposed by Inglis, Nueber and Arola-Ramulu, see Eqs. (5)–(7). In parallel, we used FE approach on COMSOL to model the roughness profiles and evaluate the SCF computationally.

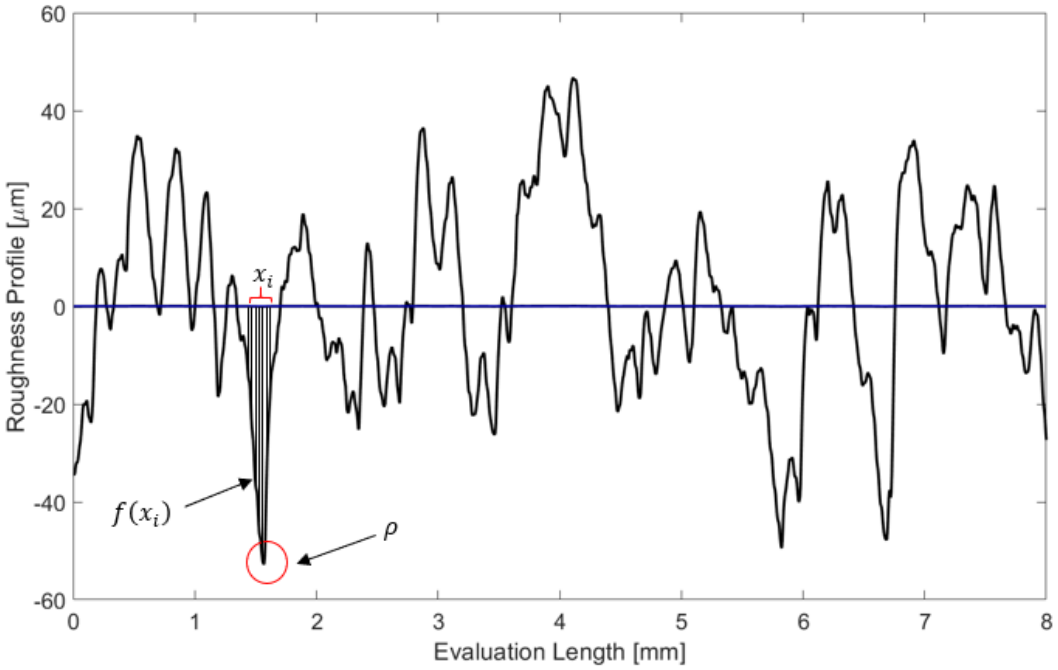


Figure 1. The surface roughness profile of the Alumec 89 block measured after the sanding process (measurement 1). The dominant valley region data points are used to compute the notch root radius.

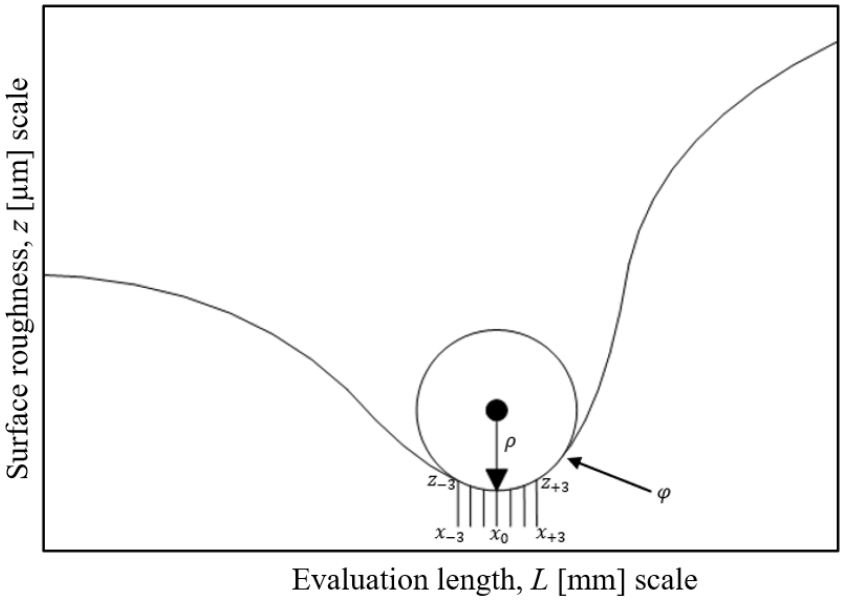


Figure 2. Geometrical correlation between radius and curvature, used for estimating the root radius of the deepest valley.

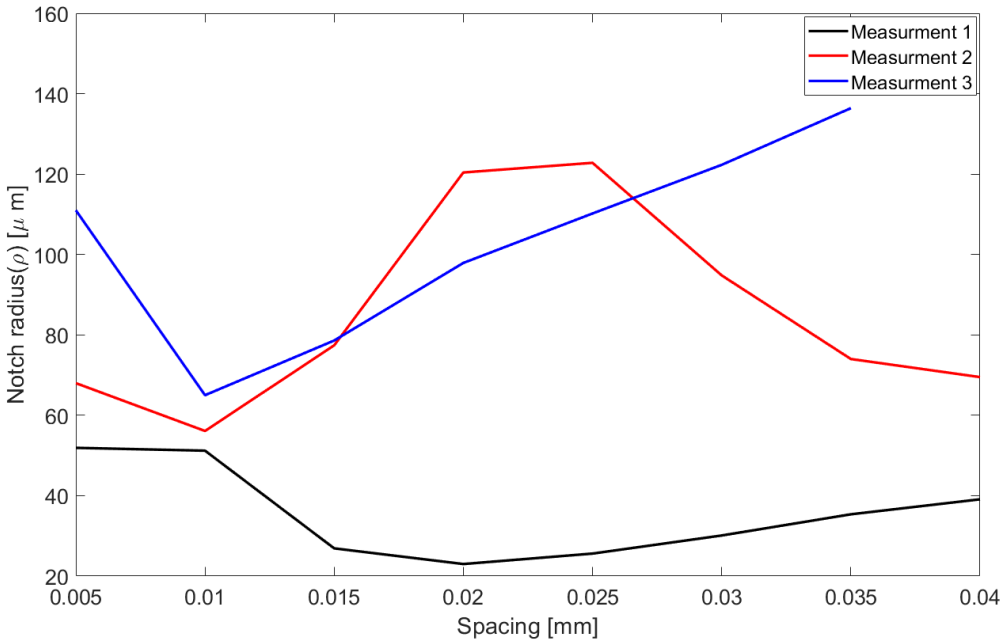


Figure 3. Calculated notch radii of the deepest valley sections with variations made on horizontal spacing, $h_i$.

## *Theoretical methods*

The methods proposed by Inglis, Neuber and Arola-Ramulu use different surface roughness parameters in SCF evaluations. These conventional surface roughness parameters are determined by roughness measurements. We used the SJ-400 surface roughness profiler and followed ISO 4287 standard for the skidless measurements. Table 1 shows parameters that are used in SCF calculations.

Table 1. Surface roughness parameters used in SCF evaluations.

| | Surface roughness parameters | | | | |
|---|---|---|---|---|---|
| | Total height $(R_t, R_y)$ | Arithmetic mean $(R_a)$ | Maximum depth $(R_v)$ | 10-point mean $(R_c, R_z)$ | Measurement |
| Values [µm] | 99.4 | 16.1 | 52.7 | 62.6 | Measurement 1 |
| Values [µm] | 106.7 | 14.7 | 69.3 | 61.6 | Measurement 2 |
| Values [µm] | 143.6 | 18.9 | 93 | 75 | Measurement 3 |

For the Neuber's method, the loading condition, $n = 2$, and spacing to asperity ratio, $\lambda = 1$ are used. For the Arola-Ramulu, the loading condition is $n = 2$, whereas, for the case of Inglis, we used the maximum depth, $R_v = a$.

## *FE analyses on COMSOL*

The raw data of the surface roughness are imported to COMSOL geometry tool to model the profile using interpolation curve function. Boundary loads of $\sigma_x = 100$ Pa and $\sigma_x = -100$ Pa are applied on the two opposite edges of the profile, with a plane-stress approximation used for the 2D structural analyses. We studied the convergence of the solutions by iteratively reducing

the element size up to $1.6e^{-6}$ mm. Fig. 4 shows the result of the von Mises stress distribution for the measurement 1, with the coordinate value superimposed.

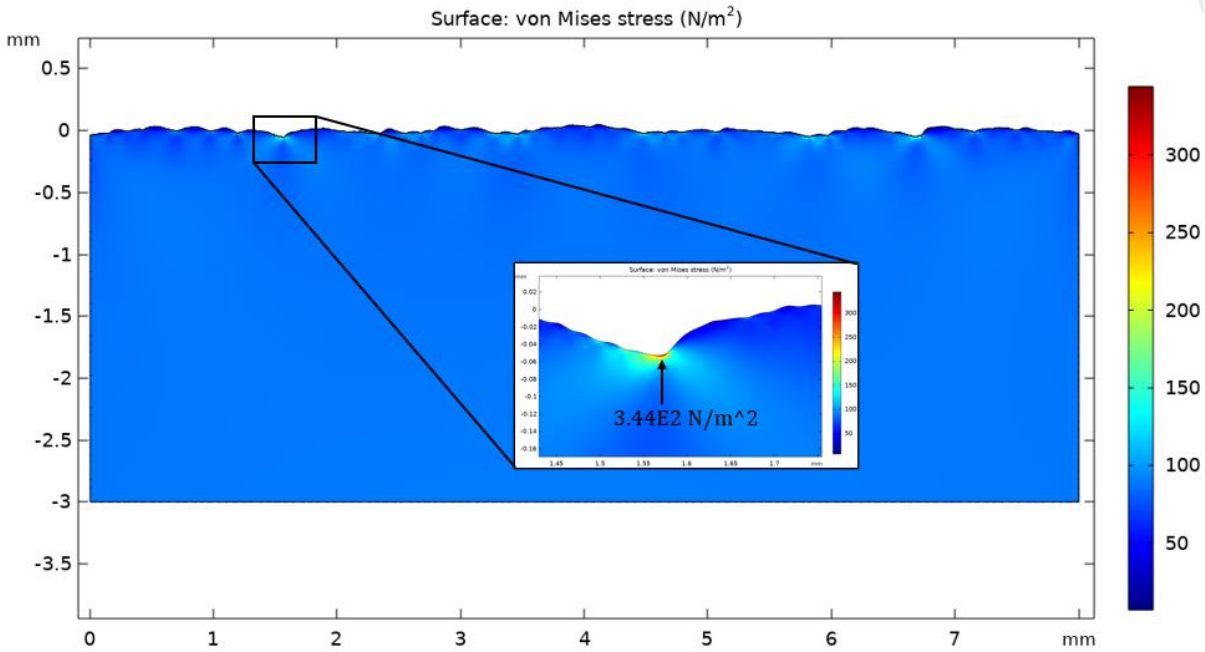


Figure 4. Von Mises stress distribution ($\sigma_v$) of the rough surface profile under a 100 Pa remote tension in the $x$ direction (Measurement 1).

For the $\sigma_x = 100$ Pa remote tensile loading, the computational method provides the stress, $\sigma_v = 344.414$ Pa at the deepest valley section. Similar computational analyses are made for the measurement 2 and measurement 3.

## Results and discussion

The theoeritical and computation approaches are used to estimate the SCF. The Neuber's and Inglis approaches showed higher SCF estimations in all the cases studied. On the other hand, the Arola-Ramulu method was better with minimum deviations. Comparing to the FE calculations, the method showed a minimum of 6.7% and a maximum of 16.3% errors for the measurements 1 and 2 respectively. Fig. 5 shows the comparisons of the SCFs evaluated using both theoretical and computation methods.

The theoretical and computational approaches provided SCFs that range between 1.96 and 4.29 for all measurements. The Neuber and Inglis approaches overestimated the SCFs and resulted in errors greater than 30% in most of the cases. Whereas, the Arola-Ramulu showed a maximum of 16.3 %. The calculated notch radius is commonly used in all theoretical calculations, however the Arola-Ramulu's showed the closest SCF estimation to the FE computations.

The Inglis approach works better for an isolated shallow notch which can be approximated to an elliptical geometry. Whereas, the Neuber's is a semi empirical approach for successively equidistant adjacent notches which have similar depth and width [16]. The Arola-Ramulu approach considers various surface roughness parameters that are inherent to the stochasticity of the profile, thus estimating SCF better than the two. The study on fatigue notch factor of a rough surface specimen by [24] also confirmed that the Arola-Ramulu estimates SCF better than the Neuber's.

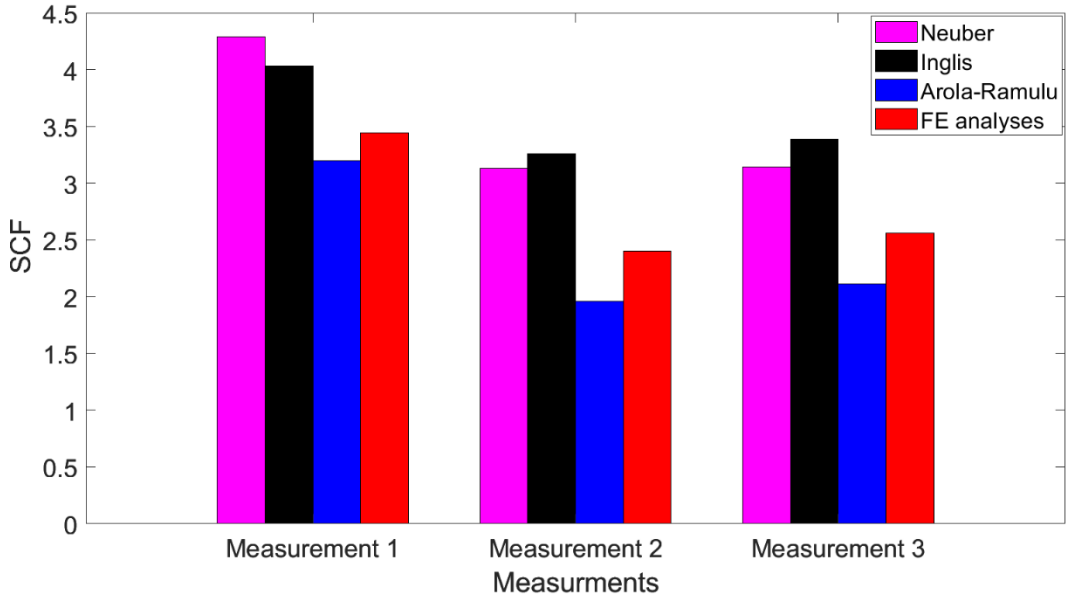


Figure 5. Calculated SCF using analytical and computational methods.

## Conclusion

The surface roughness of Alumec 89 block is measured using SJ 400 surface roughness tester to identify the dominant valley radius and estimate the SCF within the region. The theoretical and semi-empirical methods are based on the effective root radius of the region. Therefore, we used the relationship between a curvature and central difference derivatives to evaluate the radius. We calculated the SCFs using the typical approaches proposed by Inglis, Neuber and Arola-Ramulu and compared them to the FE analysis on COMSOL. The findings provide SCF values that are close to each other asserting the viability of our method in root radius estimation. Comparing the FE analysis, the Arola-Ramulu's method showed good estimation with smaller deviations. Similar conclusions are drawn in SCF comparisons by [14] on fatigue notch factor studies, and [13] on flexural strength reduction studies.

The notch radius and SCF studies have direct relevance to understand the influence of surface roughness on the fatigue strength of materials. The studies on the effect of surface roughness on fatigue strength of aluminium alloy [25], the relationship between fatigue notch factor and strength [26], and the effect of notch geometry on fatigue strength [27] emphasize the role of theoretical SCF in fatigue analyses. There exists a well-established semi empirical method that relate the theoretical SCF, with the material and geometry dependent fatigue notch factor [6, 9]. This leads to understanding the fatigue damage of components associated to deepest valleys. However, the FE analyse on the rough surface profiles showed a wide variety of stress peaks which are localized across the roughness domain. Therefore, experimental investigations would be required to study the localized fatigue phenomena of rough surface profiles.

## References

[1] Y. Murakami, *Metal Fatigue: Effect of small defect and non-metallic inclusion*, Oxford, Elsevier Science Ltd, 2002.

[2] Y.K. Gao et al., Influence of surface integrity on fatigue strength of 40CrNi2Si2MoVA steel, *Material Letter*, 61:466–468, 2006. https://doi.org/10.1016/j.matlet.2006.04.089.
[3] A. Javidi et al., The effect of machining on the surface integrity and fatigue life, *International Journal of Fatigue*, 30:2050–2055, 2008. https://doi.org/10.1016/j.ijfatigue.2008.01.005
[4] H. Remes, E. Korhonen, P. Lehto, J. Romanoff, A. Niemelä, P. Hiltunen, T. Kontkanen, Influence of surface integrity on the fatigue strength of high strength steels, *J. Construction Steel Research*, 89:21–24, 2013. https://doi.org/10.1016/j.jcsr.2013.06.003
[5] T. Stenberg, Fatigue Properties of Cut and Welded High Strength Steels – Quality Aspect in Design and Production, Doctoral Thesis, Stockholm: KTH Eng. Sc., Sweden, 2016, pp. 31–32.
[6] W.D. Pilkey and D.F. Pilkey, *Peterson's Stress Concentration Factors* (3rd ed.), New Jersey, John Wiley & Sons, 2008, Ch. 1, pp. 3–24, Ch. 2, pp. 58–68, Ch. 4, pp. 178–308.
[7] S. Z. Gebrehiwot, H. Remes, and A. T. Karttunen, A Stress concentration factor for interacting surface notch and subsurface hole, *Rakenteiden Mekaniikka*, 51:20–37, 2018. https://doi.org/10.23998/rm.70292
[8] Y. Murakami. *Theory of Elasticity and Stress Concentration*, Chichester, John Wiley & Sons, 2017, Part II, Ch. 1, pp. 248–270, Ch. 4, pp. 319–332, Ch. 5, pp. 335–337.
[9] R.E. Peterson, *Stress Concentration Factors*, New York, John Wiley & Sons, 1974, pp. 20–26.
[10] S. Khakalo and J. Niiranen, Gradient-elastic stress analysis near cylindrical holes in a plane under bi-axial tension fields, *International Journal of Solids and Structures*, 110–111:351–366, 2017. https://doi.org/10.1016/j.ijsolstr.2016.10.025
[11] D. Arola and C.L. Williams, Estimating the fatigue stress concentration factor of machined surfaces, *International Journal of Fatigue*, 24:923–928, 2002. https://doi.org/10.1016/S0142-1123(02)00012-9
[12] M. Suraratchai, J. Limido, C. Mabru and R. Chieragatti, Modelling the influence of machined surface roughness on the fatigue life of aluminium alloy, *International Journal of Fatigue*, 30:2119–2126, 2008. https://doi.org/10.1016/j.ijfatigue.2008.06.003
[13] D. Arola and M. Ramulu, An examination of the effects from surface texture on the strength of fiber reinforced plastics, *Journal of Composite Materials*, 33:102–123. https://doi.org/10.1177/002199839903300201
[14] Z. Cheng and R. Liao, Effect of surface topography on stress concentration factor, *Chin. J. Mech. Eng.*, 28:1141–1148, 2015. https://doi.org/10.3901/CJME.2015.0424.047
[15] Z. Cheng, R. Liao and W. Lu, Surface stress concentration factor via Fourier representation and its application for machined surfaces, *International Journal of Solids and Structures*, 113–114:108–117, 2017. https://doi.org/10.1016/j.ijsolstr.2017.01.023
[16] W.D. Pilkey and D.F. Pilkey, *Peterson's Stress Concentration Factors*, 3rd ed. New Jersey: John Wiley & Sons, 2008, Ch. 1, pp. 3–24, Ch. 2, pp. 58–68, Ch. 4, pp. 178–308.
[17] D.J. Whitehouse, *Handbook of Surface and Nanometrology: Surface Characterization*, Bristol, IOP Publishing Ltd, 2003.
[18] B. Bhushan, *Modern Tribology Handbook: Surface Roughness Analysis and Measurement Techniques*, vol. 1, Boca Raton, CRC Press, 2001.
[19] J.F. Song and T.V. Vorburger, *Surface Texture, ASM handbook*, vol. 18.
[20] P.L. Menezes, et al., *Tribology for Scientists and Engineers, Fundamentals of Engineering Surfaces*, New York, Springer, 2013.
[21] A. Rudawska, *5 – Mechanical Treatment, Surface Treatment in Bonding Technology*, Academic Press, 2019, pp. 87–128, ISBN 9780128170106, https://doi.org/10.1016/B978-0-12-817010-6.00005-9
[22] A.C. Fischer-Cripps, *Introduction to Contact Mechanics*, 2nd ed., New South Wales, Australia, Springer Science+Business Media, 2007.

[23] Z. Xu, *Numerical Differentiation*, University of Notre Dame, [Online]. Available: https://www3.nd.edu/~zxu2/acms40390F14/Lec-4.1.pdf [Accessed Sept. 20, 2022].
[24] Z. Cheng, R. Liao, W. Lu and D. Wang, Fatigue notch factors prediction of rough specimen by the theory of critical distance, *International Journal of Fatigue*, 104:195–205, 2017. https://doi.org/10.1016/j.ijfatigue.2017.07.004
[25] B. Zhao, J. Song, L. Xie et al., Surface roughness effect on fatigue strength of aluminum alloy using revised stress field intensity approach. *Sci Rep* 11, 19279, 2021. https://doi.org/10.1038/s41598-021-98858-0
[26] Zhi-Z. Hu and Shu-Z. Cao, Relationship between fatigue notch factor and strength, *Engineering Fracture Mechanics*, 48:127–136, 1994. https://doi.org/10.1016/0013-7944(94)90149-X
[27] X. Hu, X. Jia, Z. Bao et al., Effect of notch geometry on the fatigue strength and critical distance of TC4 titanium alloy, *J Mech Sci Technol* 31:4727–4737, 2017. https://doi.org/10.1007/s12206-017-0919-1

Silas Z. Gebrehiwot, Leonardo Espinosa-Leal
Aalto University, Department of Mechanical Engineering
Arcada University of Applied Sciences
Jan-Magnus Janssonin aukio 1, 00550 Helsinki, Finland
silas.gebrehiwot@arcada.fi, leonardo.espinosaleal@arcada.fi

Heikki Remes
Aalto University, Department of Mechanical Engineering
P.O. Box 11000, FI-00076 AALTO
heikki.remes@aalto.fi

Marinus Vermunt
Fontys University of Applied Sciences
Eindhoven, Netherlands
vermuntm@arcada.fi